A Letters Journal Exploring
the Frontiers of Physics

OFFPRINT

Phonon-roton modes in liquid ^{4}He coincide with Bose-Einstein condensation

J. Bossy, J. Ollivier, H. Schober and H. R. Glyde

EPL, **98** (2012) 56008

epl

A Letters Journal Exploring the Frontiers of Physics

EPL Compilation Index

www.epljournal.org

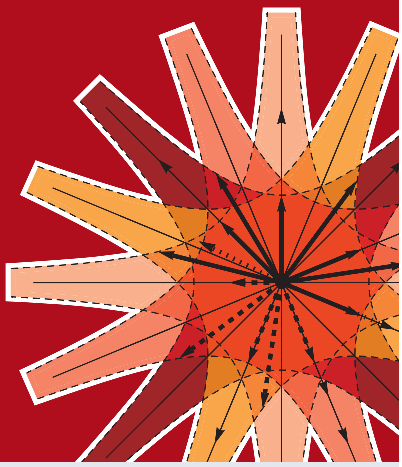

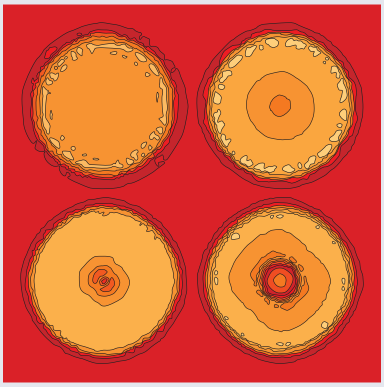
Biaxial strain on lens-shaped quantum rings of different inner radii, adapted from **Zhang *et al*** 2008 EPL **83** 67004.

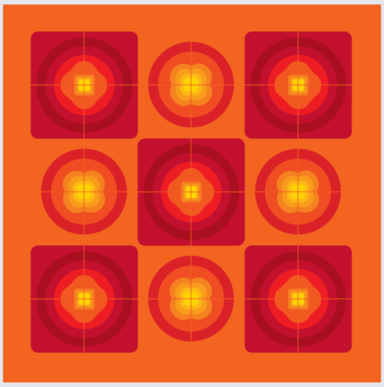
Artistic impression of electrostatic particle–particle interactions in dielectrophoresis, adapted from **N Aubry and P Singh** 2006 *EPL* **74** 623.

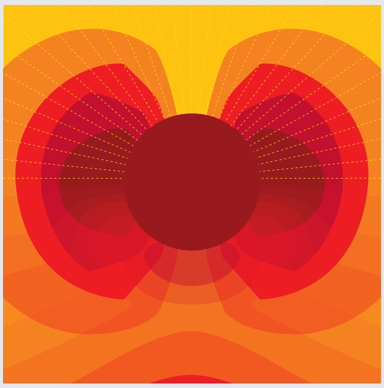
Artistic impression of velocity and normal stress profiles around a sphere that moves through a polymer solution, adapted from **R Tuinier, J K G Dhont and T-H Fan** 2006 *EPL* **75** 929.

Visit the EPL website to read the latest articles published in cutting-edge fields of research from across the whole of physics.

Each compilation is led by its own Co-Editor, who is a leading scientist in that field, and who is responsible for overseeing the review process, selecting referees and making publication decisions for every manuscript.

- Graphene
- Liquid Crystals
- High Transition Temperature Superconductors
- Quantum Information Processing & Communication
- Biological & Soft Matter Physics
- Atomic, Molecular & Optical Physics
- Bose–Einstein Condensates & Ultracold Gases
- Metamaterials, Nanostructures & Magnetic Materials
- Mathematical Methods
- Physics of Gases, Plasmas & Electric Fields
- High Energy Nuclear Physics

If you are working on research in any of these areas, the Co-Editors would be delighted to receive your submission. Articles should be submitted via the automated manuscript system at **www.epletters.net**

If you would like further information about our author service or EPL in general, please visit **www.epljournal.org** or e-mail us at **info@epljournal.org**

EPS Società Italiana di Fisica EDP SCIENCES **IOP** Publishing

Image: Ornamental multiplication of space-time figures of temperature transformation rules (adapted from T. S. Bíró and P. Ván 2010 *EPL* **89** 30001; artistic impression by Frédérique Swist).

A Letters Journal Exploring the Frontiers of Physics

June 2012

EPL, **98** (2012) 56008
www.epljournal.org
doi: 10.1209/0295-5075/98/56008

Phonon-roton modes in liquid ^{4}He coincide with Bose-Einstein condensation

J. Bossy[1], J. Ollivier[2], H. Schober[2,3] and H. R. Glyde[4]

[1] *Institut Néel, CNRS-UJF - BP 166, F-38042 Grenoble Cedex 9, France, EU*
[2] *Institut Laue-Langevin - BP 156, F-38042 Grenoble, France, EU*
[3] *Université Joseph Fourier, UFR de Physique - F-38041 Grenoble Cedex 9, France, EU*
[4] *Department of Physics and Astronomy, University of Delaware - Newark, DE 19716-2593, USA*

received 11 February 2012; accepted in final form 15 May 2012
published online 13 June 2012

PACS 61.05.fg – Neutron scattering (including small-angle scattering)
PACS 67.10.Ba – Boson degeneracy
PACS 67.25.dr – Restricted geometries

Abstract – We present neutron scattering measurements of the phonon-roton (P-R) and layer modes of liquid ^{4}He confined in MCM-41 under pressure up to 38 bar. The data shows unambiguously that the P-R mode exists at low temperature only. As temperature is increased, there is a gradual transfer of intensity from the P-R mode to the normal liquid response, which lies at a lower energy at higher pressure. The transfer takes place with no observable mode broadening. The loss of P-R modes is identified with the loss of Bose-Einstein condensation (BEC). The mode giving rise to the specific heat, c_V, of liquid ^{4}He in porous media (*e.g.*, gelsil) at higher temperature is the layer mode since the energy of the mode extracted from c_V and the layer mode energy are the same.

There is a rich and long-standing debate on the nature of phonon-roton (P-R) modes in liquid ^{4}He. The first picture is that they are collective density modes of a strongly interacting cold Bose liquid. This picture was initiated by Landau [1,2] and developed by Feynman [3] and others [4–7]. It forms the basis used today to calculate P-R mode energies with high accuracy [8–10]. In this picture gradual thermal broadening of modes with increasing temperature is expected [11–14]. The second is that they are density modes but Bose-Einstein condensation (BEC) plays a critical role in establishing them as sharply defined modes at low temperature, especially at higher wave vectors in the roton region $Q \simeq 2\,\text{Å}^{-1}$ and beyond. When there is BEC, the density and single-particle (SP) modes have the same energy [15–18]. There are therefore no independent, low-energy SP modes to which the P-R mode can decay. The P-R mode can decay only to itself, which becomes vanishingly small at low temperature. This picture originated with Bogoliubov [15] and was extended to Bose liquids by Gavoret and Nozières [16] and others [17,18]. The single-particle and density responses observed in the dynamic structure factor, $S(Q,E)$, are coupled via the condensate. In this picture we expect a difference [19] in S(Q, E) below and above T_{BEC}, the temperature at which BEC vanishes and above which independent SP modes can exist.

We present new data on liquid ^{4}He under pressure in MCM-41 which shows that the P-R mode at higher wave vectors exists at low temperature only. As the temperature is increased, there is a transfer of intensity from the P-R mode to new intensity at low energy. Above a specific temperature, denoted T_{BEC}, there is no longer an observable P-R mode. T_{BEC} is identified as the temperature at which BEC and as a result P-R modes no longer exist in the liquid. Above T_{BEC}, all the intensity is at low energy, which is interpreted as the response of the normal liquid (NL) where there is no BEC.

A simple transfer of intensity from the P-R mode to NL response with no mode broadening is observed at 34 bar because, under pressure, a) the P-R mode disappears at low temperature ($T_{BEC} \simeq 1.5\,\text{K}$) before thermal broadening of the mode becomes significant and b) the "normal" liquid response lies at low energy ($E \simeq 0$) that can be readily distinguished from the P-R mode. The P-R mode is therefore not simply a sharp density mode in a cold Bose liquid which broadens with increasing temperature. Rather it depends for its existence as a sharp mode on BEC. The transfer of intensity is not so clear in bulk liquid ^{4}He at lower pressure because there is mode broadening as well as intensity transfer and the P-R and NL intensities overlap in energy making it difficult to distinguish the NL response from the broadened P-R mode. In the bulk liquid, the loss of BEC coincides with the loss of superflow ($T_{BEC} = T_\lambda$). Above T_{BEC}, the normal liquid response in bulk liquid ^{4}He changes little with temperature [20,21].

Secondly we present measurements of the layer modes in liquid ^{4}He under pressure in both MCM-41 and gelsil. This shows that the mode responsible for the specific heat, c_V, of liquid helium in porous media at higher pressure is the layer mode, as at SVP in Vycor [22–24]. Thus, the temperature at which c_V peaks is governed by the layer mode and the existence of layer modes has no established connection with BEC.

The measurements were performed on the IN5 and IN6 time-of-flight spectrometers at the Institut Laue-Langevin which are described fully at `www.ill.fr`. Incident neutron wavelengths of 5.0 Å and 4.1 Å, with corresponding energy resolutions of 0.1 meV and 0.17 meV, were used, respectively. The MCM-41 of 47 ± 3 Å pore diameter was fabricated by the "Laboratoire de Materiaux Mineraux", Mulhouse, France, and is fully described in ref. [25]. The gelsil of 25 Å mean pore diameter was fabricated by 4F International and is fully described in ref. [26]. In these porous media, ^{4}He remains liquid up to 38 bar where it solidifies to an amorphous solid [25]. The sample cells are fully described in refs. [25,26].

Figure 1 (top) shows the scattering intensity, proportional to the dynamic structure factor, $S(Q,E)$, from the helium in the sample cell at 25.3 bar and $T = 0.4$ K. This is scattering from the liquid ^{4}He in the MCM-41 pores and the bulk crystalline solid ^{4}He between the grains of the MCM-41. The volume in the pores and between the grains is $V_P = 0.83\,\text{cm}^3$ and $V_{IG} = 1.87\,\text{cm}^3$, respectively, $V_P/V_{IG} = 0.44$. The helium in the pores is liquid except the first 1–2 layers on the pore walls which is amorphous solid. Elastic scattering from the amorphous solid layers is seen in fig. 1 at $E = 0$ and $1.8 < Q < 2.5\,\text{Å}^{-1}$. The P-R mode of the liquid ^{4}He in the MCM-41 pores is observed at energies, $0.6 \lesssim E \lesssim 1.2$ meV. The P-R dispersion curve is only faintly visible in the phonon region ($Q \simeq 0.5\,\text{Å}^{-1}$), not visible in the "maxon" region ($Q \simeq 1.1\,\text{Å}^{-1}$) but is intense in the roton region, $1.8 \leqslant Q \leqslant 2.3\,\text{Å}^{-1}$ and $E \simeq 0.6$ meV. The intensity at higher energy arises from phonons in the polycrystalline solid between the grains. The lower-energy optic phonons in the polycrystalline solid have an apparent "roton"-like appearance at an energy $E \simeq 1.1$ meV on a time-of-flight instrument.

Figure 1 (bottom) shows the scattering intensity, $S(Q,E)$, at fixed wave vector $Q = 2.10\,\text{Å}^{-1}$ (the roton Q) *vs.* E as a function of pressure at $T = 0.4$ K. The large peak at $E \simeq 0$ is the elastic scattering. The peak at $E \simeq 0.6$ meV arises from the roton in the liquid confined in the MCM-41 pores and that at $E = 1.1$–1.4 meV from the phonons in the bulk solid around the MCM-41.

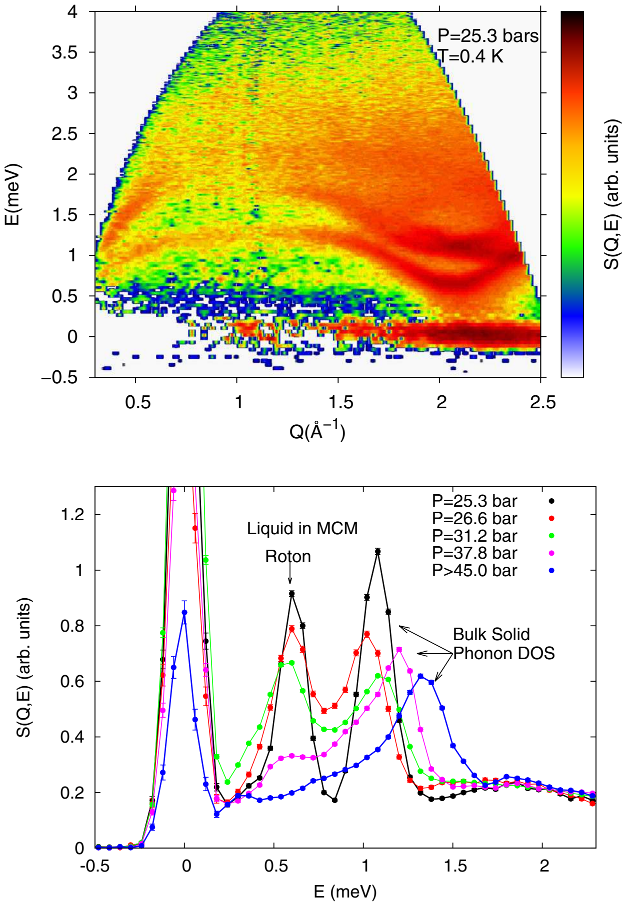

Fig. 1: (Colour on-line) Top: neutron scattering intensity, $S(Q,E)$, from liquid ^{4}He in the MCM-41 pores and from the bulk solid helium between the grains of the MCM-41 as a function of momentum (Q) and energy (E) transfer. There is elastic scattering at $E = 0$ and $1.8 \leqslant Q \leqslant 2.5\,\text{Å}^{-1}$, inelastic scattering from the phonon-roton (P-R) mode of liquid ^{4}He in MCM-41, especially in the roton region ($Q \simeq 1.8$–$2.3\,\text{Å}^{-1}$) centered at $E \simeq 0.6$ meV, and inelastic scattering from phonons in bulk solid helium, particularly for $1.8 \leqslant Q \leqslant 2.3\,\text{Å}^{-1}$ and $E \simeq 1.1$ meV. Bottom: $S(Q,E)$ at constant $Q = 2.1\,\text{Å}^{-1}$ (the roton Q) *vs.* pressure at $T = 0.4$ K. The intensity arising from the roton of liquid ^{4}He in MCM-41 decreases with increasing pressure until at 37.8 bar there is little or no roton.

As pressure is increased, the intensity in the roton peak decreases until at $p = 37.8$ bar there is essentially no roton peak. Immediately above 37.8 bar, the liquid solidifies [25]. At $p > 45$ bar, where there is amorphous solid in the pores [25], no roton is observed. The roton energy decreases with increasing pressure, as in bulk liquid ^{4}He [21,27]. In contrast the energy of the phonon density of states (DOS) increases with increasing pressure as expected in an ordinary solid. The key result is that the roton intensity decreases gradually with increasing pressure and there is no roton in the solid phase, $p > 38$ bar.

Figure 2 shows the net scattering intensity, $S(Q,E)$, at $Q = 2.1\,\text{Å}^{-1}$ from the liquid in the MCM-41 pores at 34 bars and low temperature, $T = 0.2$ K. The scattering from

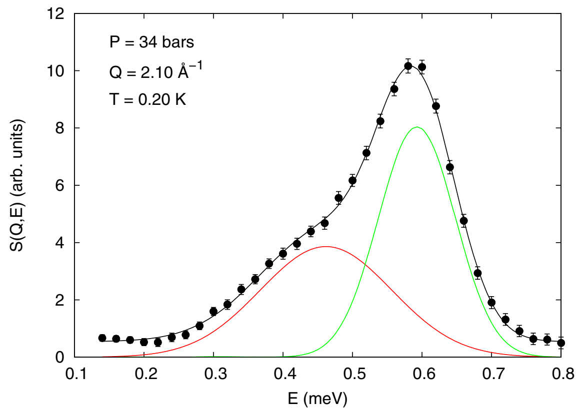

Fig. 2: (Colour on-line) Net $S(Q,E)$ of liquid ^{4}He confined in MCM-41 at 34 bar and $T = 0.2$ K (solid circles) at the roton wave vector, $Q = 2.1$ Å^{-1}, *vs.* E. Also shown is a fit consisting of a phonon-roton mode, $S_R(Q,E)$, (green line centered at $E \simeq 0.6$ meV) and a layer mode, $S_L(Q,E)$, (red line centered at $E \simeq 0.45$ meV), $S(Q,E) = S_R(Q,E) + S_L(Q,E)$.

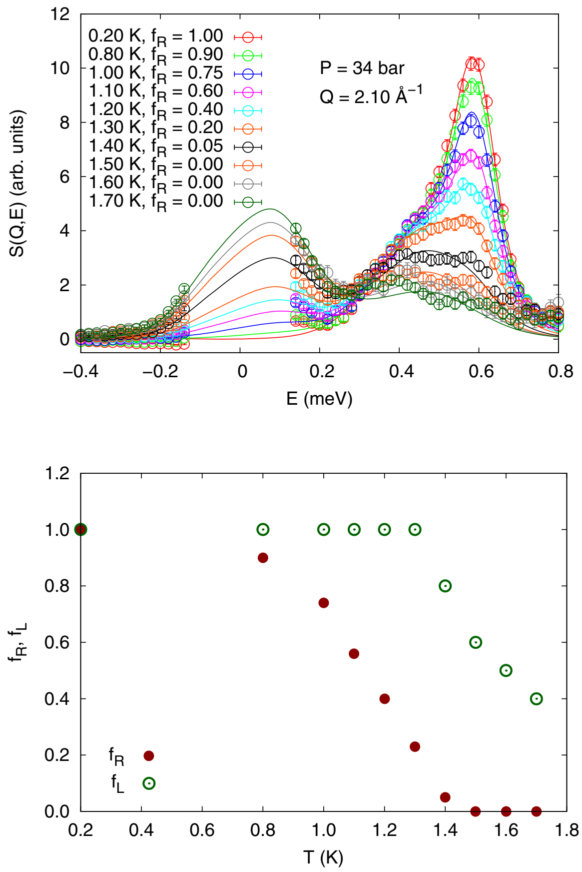

Fig. 3: (Colour on-line) Top: net $S(Q,E)$ of liquid ^{4}He confined in MCM-41 at $Q = 2.1$ Å^{-1} *vs.* temperature at constant pressure $p = 34$ bar (open circles). Also shown are fits (lines) to the data using the model in eqs. (3) and (4) in which $S_R(Q,E)$, $S_N(Q,E)$ and $S_L(Q,E)$ are all independent of T. The temperature dependence in eqs. (3) and (4) arises from allowing the weights f_R and f_L in the P-R mode and layer mode to decrease with T. At $T = 0.2$ K, $f_R = f_L = 1$. Bottom: the weights, f_R and f_L in the P-R mode and layer mode, respectively, *vs.* temperature. Up to 1.3 K, $f_L = 1$. The weight in the P-R mode goes to zero at $T = 1.5$ K.

the amorphous solid layers on the pore walls and the solid between the MCM-41 grains has been subtracted. The net liquid $S(Q,E)$ can be fitted as the sum of two modes, a roton mode, $S_R(Q,E)$, centered at $E \simeq 0.6$ meV plus a broad layer mode, $S_L(Q,E)$, peaked at $E \simeq 0.45$ meV as shown in fig. 2. More complex representations of $S(Q,E)$ are possible. A P-R mode and a broad layer mode (which could be more than one layer mode [28]) are observed widely in porous media such as Vycor [29–31] and aerogel [32]. The layer mode propagates in the 2–4 layers of liquid closest to the pore walls. The P-R mode, the same mode as found in bulk liquid helium, propagates in these layers and in the liquid in the interior of the media. The association of layer modes with the liquid layers near the walls and P-R modes chiefly with the liquid in the interior is determined from measurements of mode intensities as a function of filling [32].

Specifically, we write

$$S(Q,E) = S_R(Q,E) + S_L(Q,E), \qquad (1)$$

in which the roton mode $S_R(Q,E)$ is represented by a damped harmonic oscillator (DHO) function,

$$S_R(Q,\omega) = (Z_Q/\pi)[n_B(\omega)+1] \times \left[\frac{\Gamma_Q}{(\omega-\omega_Q)^2+\Gamma_Q^2} - \frac{\Gamma_Q}{(\omega+\omega_Q)^2+\Gamma_Q^2}\right], \qquad (2)$$

where $n_B(\omega)$ is the Bose function, and $S_L(Q,E)$ by a Gaussian function. A best fit to the data in fig. 2 gives a roton energy $\omega_Q = 0.59 \pm 0.02$ meV and width $2\Gamma_Q = 0.071 \pm 0.004$. Interestingly, the roton has a finite apparent intrinsic width in MCM-41 at 34 bar at $T = 0.20$ K.

The magnitude of $S_L(Q,E)$ in eq. (1) depends on the volume of liquid in the liquid layers near the walls. From the fits to the data in fig. 2, we found integrated intensities of $S_R(Q) = 1.08$ and $S_L(Q) = 0.91$. This means that in MCM-41 the volume of liquid near the walls is large enough that $S_L(Q)$ is comparable to $S_R(Q)$. In large pore media $S_L(Q)$ is relatively much smaller [32]. Note that while there is some overlap, the roton and layer modes propagate in different regions of the liquid.

Figure 3 (top) shows the temperature dependence of the net $S(Q,E)$ at 34 bar. In fig. 3, the intensity from the solid at $T = 0.2$ K that was subtracted was multiplied by the thermal factor $[n_B(\omega)+1]$ to allow for the temperature dependence of the background, a negligible effect for $E > 0.15$ meV up to 1.7 K. As temperature is increased, the intensity in the P-R mode decreases. The intensity that was in the P-R mode at low temperature is transferred to new intensity at low energy centered near $E \simeq 0$ at higher temperatures. At $T = 1.5$ K the P-R mode is no longer observed, as we show below. This is similar to the transfer of intensity seen in the bulk liquid at lower pressure [20,33,34]. However, it is much clearer in the present data at 34 bars for two reasons. Firstly in fig. 3 (top), the transfer of intensity takes place with no observable thermal broadening of the P-R mode. This is because the roton has already a small intrinsic width, $2\Gamma_Q = 0.07$ meV at low temperature ($T = 0.20$ K), and the roton intensity vanishes at $T = 1.5$ K where the thermal broadening of the roton mode is small [20] (*e.g.*, in bulk liquid ^{4}He at 20 bars at $T = 1.5$ K, $2\Gamma_Q \simeq 0.08$ meV). Thus, it is clear that the temperature dependence is intensity loss without broadening. Secondly, as temperature increases, the intensity lost from the P-R mode appears at low energy near $E \simeq 0$ well separated from the P-R mode. The layer mode survives to higher temperature, above 1.7 K, the maximum temperature investigated here.

As in earlier work [30,35–38], we interpret the temperature at which the roton disappears as T_{BEC}, the maximum temperature at which BEC exists in the liquid. Thus, at 34 bar $T_{BEC} = 1.5$ K. At SVP, the P-R mode in porous media exists up to a temperature T_{BEC} which lies below but is close to T_λ in all media investigated [30,35,37,39,40]. At higher pressure (*e.g.*, 32–34 bar), T_{BEC} is reduced to about 1.5 K in all porous media investigated (Vycor, gelsils and MCM-41) [26,38,41]. While T_{BEC} is similar in all porous media, the superfluid transition temperature T_c is very sensitive to the pore geometry and size [24,42–44] and lies below T_{BEC}. For example, T_c goes to zero at 34 bar in 25 Å gelsil [43] where $T_{BEC} \simeq 1.5$ K. The temperature range $T_c < T < T_{BEC}$, where there is BEC but no superflow, is interpreted as a temperature range of localized BEC [30,35–38,45] in which the BEC is spatially localized to islands (*e.g.*, 25 Å in diameter) separated by normal liquid.

The new feature of the present data in fig. 3 is that the intensity in the P-R mode decreases as temperature is increased without observable mode broadening and this intensity is transferred to new response centered near $E \simeq 0$. The intensity near $E \simeq 0$ is interpreted as normal liquid response, $S_N(Q,E)$. Thus, the present data shows that the temperature dependence of $S(Q,E)$ is not a broadening of the P-R mode. Rather, $S(Q,E)$ below and above T_{BEC} is quite different and lies in a different energy range.

To clarify the temperature dependence of $S(Q,E)$ in fig. 3 (top) we fitted a simple model to the data consisting of a P-R mode, $S_R(Q,E)$, a layer mode, $S_L(Q,E)$, and the normal liquid response, $S_N(Q,E)$. The $S_R(Q,E)$, $S_L(Q,E)$ and $S_N(Q,E)$ are all assumed to be independent of temperature. In the model only the weights in the modes change with temperature. The weights f_R and f_L, in $S_R(Q,E)$ and $S_L(Q,E)$, respectively, decrease with temperature and this weight is transferred to $S_N(Q,E)$. The weights f_R and f_L are obtained by fits to data as a function of temperature. Up to $T = 1.3$ K we can get a good fit to the data with a model in which there is transfer from the roton to the normal liquid response only, *i.e.*, only f_R changes with temperature with the weight in the layer mode independent of T,

$$S(Q,E) = [f_R(T)S_R(Q,E) + (1 - f_R(T))S_N(Q,E)] + S_L(Q,E)]. \quad (3)$$

The fits of eq. (3) to data up to $T = 1.3$ K are shown as lines in fig. 3 (top) and the best-fit values of f_R are shown in fig. 3 (bottom).

Above 1.3 K, between 1.4 K and 1.7 K, the maximum temperature investigated, we obtain a better fit if the weight f_L in the layer mode also decreases with T. That is, above 1.3 K we expand the model to

$$S(Q,E) = [f_R(T)S_R(Q,E) + (1 - f_R(T))S_N(Q,E)] + [f_L(T)S_L(Q,E) + (1 - f_L(T))S_N(Q,E)], \quad (4)$$

in which there is in addition transfer of intensity from the layer mode to $S_N(Q,E)$. The best fit values of f_R and f_L are again shown in fig. 3 (bottom). We see that the weight in the P-R mode f_R decreases uniformly with increasing temperature and $f_R = 0$ at $T = 1.5$ K. The temperature dependence of f_R is similar to that of the condensate fraction [46], $n_0(T)$. The integrated intensity in the normal response is $S_N(Q) = 1.10$ so that, with $S_R(Q) = 1.08$ and $S_L(Q) = 0.91$, the total $S(Q)$ of the model eq. (4) is approximately independent of temperature as observed in bulk liquid ^{4}He. These fits confirm that there is a complete transfer of intensity from the P-R mode at low T to normal liquid response centered at $E \simeq 0$ at $T_{BEC} = 1.5$ K and that $S(Q,E)$ is quite different above and below T_{BEC}.

To illustrate how BEC can play a role in establishing well defined P-R modes in $S(Q,E)$ we turn to the field theory formulation [15–18] of $S(Q,E)$ in which n_0 appears explicitly. In this formulation both the single-particle Green function, $G(Q,\omega)$, and the density dynamical susceptibility, $\chi(Q,\omega)$, that we observe in $S(Q,\omega)$, are evaluated. Specifically, $S(Q,\omega)$ is given by $S(Q,\omega) = -(1/\pi)[n_B(\omega)+1]\chi''(Q,\omega)$, where χ'' is the imaginary part of χ. When there is a condensate, $\chi(Q,\omega)$ and $G(Q,\omega)$ have a common denominator [17] and therefore have the same poles and mode energies. There is only a single joint density/single-particle mode. Thus there are no independent single-particle modes lying at low energy to which the density P-R mode can decay. As a result the P-R mode is uniquely sharply defined at low temperature (*e.g.*, compared to phonons in solid ^{4}He or zero sound in normal liquid ^{3}He). We expect sharply defined modes below T_{BEC} where there is BEC but not above T_{BEC} where there will be independent single-particle modes.

Secondly, when there is a condensate, the single particle $G(Q,\omega)$ appears in $\chi(Q,\omega)$ with a weight proportional to n_0. This may be seen qualitatively from the intermediate DSF,

$$S(\mathbf{Q},t) = \frac{1}{N}\langle \rho(\mathbf{Q},t)\,\rho^\dagger(\mathbf{Q},0)\rangle,$$

where $\rho^\dagger(\mathbf{Q}) = \sum_k a^\dagger_{k+Q} a_k$ is the density operator and $a^\dagger_k$ is the single-particle creation operator. When there is a condensate (macroscopic occupation of the $k=0$ state), the a_0 becomes a number, $a_0 = \sqrt{N_0}$ and $a_0^\dagger = \sqrt{(N_0+1)} \simeq \sqrt{N_0}$ where $n_0 = N_0/N$. Thus, $\rho^\dagger(\mathbf{Q}, 0)$ separates as

$$\rho^\dagger(\mathbf{Q}) = \sqrt{N_0} A_Q^\dagger + \rho'^\dagger(\mathbf{Q}), \tag{5}$$

where $A_Q^\dagger = a_Q^\dagger + a_{-Q}$ and $\rho'(\mathbf{Q})$ is the "regular" density operator that does not include the $k=0$ state. In this case

$$\chi(Q,\omega) = n_0 G(Q,\omega) + \chi_{INT}(Q,\omega) + \chi_R'(Q,\omega) \tag{6}$$

in which first term is proportional to n_0 and $\chi_{INT}(Q,\omega)$ is a cross term proportional to $\sqrt{n_0}$.

When the P-R mode energy is high and near the edge of the two P-R band, the weight in the P-R mode is small. This is the case at higher wave vectors beyond the roton, $Q \geqslant 2.5$ Å^{-1}. At wave vectors beyond the roton, eq. (6) for $\chi(Q,\omega)$ describes the temperature dependence of $S(Q,E)$ well [47]. The sharp mode is represented by the $G(Q,\omega)$ term with weight in $S(Q,\omega)$ proportional to the condensate fraction, $n_0(T)$, which tracks the observed weight in the P-R mode well. The sharp P-R mode is no longer observed [48] above T_{BEC} where $n_0 = 0$.

In the present data, the weight of the roton in $S(Q,E)$ appears to be proportional to $n_0(T)$. However, at the roton wave vector, as in bulk liquid helium, almost all of the weight in $S(Q,E)$ lies in the roton mode. At the same time, n_0 is small, especially at high pressure (less than 3%). In this case the simple model equation (6) would not reproduce the present data. Somehow there must be a transfer of intensity into the P-R mode from the remainder of $\chi(Q,\omega)$. Thus, at this stage, the field-theoretic formulation of $S(Q,E)$ provides a framework for understanding why the intensity in the roton can be proportional to n_0 and why the response is very different below and above T_{BEC}. However, an explicit model that reproduces the data of fig. 3 remains to be constructed.

Finally, as noted above, liquid ^{4}He in porous media and in films on surfaces supports layer modes that propagate in the liquid layers adjacent to the media walls. The layer mode is observed at wave vectors $1.7 < Q < 2.3$ Å^{-1} and has a roton-like energy minimum, Δ_L, at an energy approximately 0.15 meV below the P-R roton energy, Δ. Figure 4 shows the roton energy, Δ, in MCM-41 and the layer mode energy, Δ_L, in MCM-41 and gelsil observed here *vs.* pressure. The Δ in MCM-41 and in gelsil [38,41] are consistent with bulk roton energies [21,49]. Indeed, in all porous media investigated to date, the P-R mode energies are found to be the same as those in the bulk within precision at SVP [32] and at higher pressure [38,41]. As shown initially in Vycor, it is the excitation of the lower-energy layer mode that is responsible for the specific heat of liquid ^{4}He at high temperature in porous media [24]. For example, in early measurements [22] at SVP in Vycor, c_V was identified as arising from excitation of a layer mode. The layer mode energy extracted from c_V ($\Delta_L = 0.53 \pm 0.02$ meV) agrees with the layer

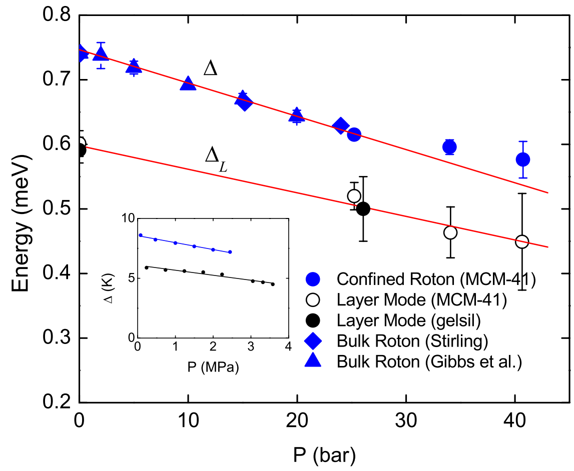

Fig. 4: (Colour on-line) The roton and layer mode energies *vs.* pressure. The blue symbols are the roton energies (Δ); triangles and diamonds in bulk liquid ^{4}He at $p \leqslant 24$ bar (from Gibbs *et al.* [21] and Stirling [49]) and solid circles in MCM-41 ($25 < p < 40$ bar). The roton energy in all porous media investigated is the same as in the bulk [32,39]. The solid and open black circles are the layer mode energies (Δ_L) in gelsil and MCM-41, respectively. In the inset, the upper line is the bulk roton energy and the lower line the energy of the mode extracted by Yamamoto [45] from the c_V of liquid ^{4}He in gelsil, which agrees with the layer mode energy Δ_L that we observe here (inset from Yamamoto *et al.* [45]). (1 meV = 11.6 K.)

mode energy subsequently observed in Vycor [29,30] ($\Delta_L = 0.55 \pm 0.01$ meV).

The inset in fig. 4 shows both the bulk roton energy Δ and the energy of the mode extracted from c_V in gelsil [45] which lies below Δ. The energy of the mode extracted [45] from c_V agrees well with the layer mode energy, Δ_L observed here, as was the case in Vycor at SVP. For this reason we believe, it is excitation of the layer mode and not the P-R mode that gives rise to c_V at high temperature in gelsil. If this is the case, then the temperature at which c_V peaks is determined by the layer mode energy and is not related to the P-R mode. The temperature at which c_V peaks has been used to identify T_{BEC}. However, there is no demonstrated connection between the existence of layer modes and BEC. For this reason, the c_V in porous media has, at this time, no demonstrated connection with BEC or T_{BEC}.

In summary, the present data shows that the P-R mode of liquid ^{4}He at higher Q values exists only at low temperature. As temperature is increased, the weight in the P-R mode decreases and this weight is transferred from the P-R mode to new response at low energy, interpreted as normal liquid (NL) response. The transfer of intensity takes place with no observable mode broadening because the temperature is low. The normal liquid response lies at low energy well below the P-R mode. The temperature at which the P-R mode vanishes is identified as T_{BEC}, the temperature at which the liquid no longer supports localized patches of BEC and becomes a fully normal liquid. An independent measurement of the condensate fraction, $n_0(T)$ in MCM-41 to confirm T_{BEC} would be most interesting but is difficult. The temperature dependence of the weight in the below T_{BEC} is similar to that of the condensate fraction $n_0(T)$ observed in bulk ^{4}He and a connection between n_0 and this weight is made.

***

It is a pleasure to acknowledge the support of the Institut Laue-Langevin and O. Losserand and X. Tonon at ILL for valuable assistance with the experiments. This work was supported by the US DOE, Office of Basic Energy Sciences under Contract No. ER46680.

REFERENCES

[1] Landau L. D., *J. Phys. USSR*, **5** (1941) 71.
[2] Landau L. D., *J. Phys. USSR*, **11** (1947) 91.
[3] Feynman R. P., *Phys. Rev.*, **94** (1954) 262.
[4] Feynman R. P. and Cohen M., *Phys. Rev.*, **102** (1956) 1189.
[5] Lee D. K. and Lee F. J., *Phys. Rev. B*, **11** (1975) 4318.
[6] Manousakis E. and Pandharipande V. R., *Phys. Rev. B*, **33** (1986) 150.
[7] Krotscheck E., *J. Low Temp. Phys.*, **113** (1998) 509.
[8] Ceperley D. M., *Rev. Mod. Phys.*, **67** (1995) 279.
[9] Boronat J. and Casulleras J., *Europhys. Lett.*, **38** (1997) 291.
[10] Boninsegni M., Prokof'ev N. V. and Svistunov B. V., *Phys. Rev. Lett.*, **96** (2006) 070601.
[11] Landau L. D. and Khalatnikov I. M., *Zh. Eksp. Teor. Fiz.*, **19** (1949) 637.
[12] Khalatnikov I. M., *Introduction to the Theory of Superfluidity* (Benjamin, New York) 1965.
[13] Svensson E. C., Montfrooij W. and de Schepper I. M., *Phys. Rev. Lett.*, **77** (1996) 4398.
[14] Montfrooij W. and Svensson E. C., *J. Low Temp. Phys.*, **121** (2000) 293.
[15] Bogoliubov N. N., *J. Phys. USSR*, **11** (1947) 23.
[16] Gavoret J. and Nozières P., *Ann. Phys. (N.Y.)*, **28** (1964) 349.
[17] Griffin A., *Excitations in a Bose Condensed Liquid* (Cambridge University Press, Cambridge) 1993.
[18] Glyde H. R., *Excitations in Liquid and Solid Helium* (Oxford University Press, Oxford) 1994.
[19] Glyde H. R. and Griffin A., *Phys. Rev. Lett.*, **65** (1990) 1454.
[20] Talbot E. F., Glyde H. R., Stirling W. G. and Svensson E. C., *Phys. Rev. B*, **38** (1988) 11229.
[21] Gibbs M. R., Andersen K. H., Stirling W. G. and Schober H., *J. Phys.: Condens. Matter*, **11** (1999) 603.
[22] Brewer D. F., Symonds A. J. and Thomson A. L., *Phys. Rev. Lett.*, **15** (1965) 182.
[23] Brewer D. F., *J. Low Temp. Phys.*, **3** (1970) 205.
[24] Reppy J. D., *J. Low Temp. Phys.*, **87** (1992) 205.
[25] Bossy J., Hansen T. and Glyde H. R., *Phys. Rev. B*, **81** (2010) 184507.
[26] Bossy J., Pearce J. V., Schober H. and Glyde H. R., *Phys. Rev. B*, **78** (2008) 224507.
[27] Stirling W. G. and Glyde H. R., *Phys. Rev. B*, **41** (1990) 4224.
[28] Clements B. E., Godfrin H., Krotscheck E., Lauter H. J., Leiderer P., Passiouk V. and Tymczak C. J., *Phys. Rev. B*, **53** (1996) 12242.
[29] Dimeo R. M., Sokol P. E., Anderson C. R., Stirling W. G., Andersen K. H. and Adams M. A., *Phys. Rev. Lett.*, **81** (1998) 5860.
[30] Glyde H. R., Plantevin O., Fak B., Coddens G., Danielson P. S. and Schober H., *Phys. Rev. Lett.*, **84** (2000) 2646.
[31] Albergamo F., Glyde H. R., Daughton D. R., Mulders N., Bossy J. and Schober H., *Phys. Rev. B*, **69** (2004) 014514.
[32] Fåk B., Plantevin O., Glyde H. R. and Mulders N., *Phys. Rev. Lett.*, **85** (2000) 3886.
[33] Andersen K. H. and Stirling W. G., *J. Phys.: Condens. Matter*, **6** (1994) 5805.
[34] Zsigmond G., Mezei F. and Telling M. T. F., *Physica B*, **388** (2007) 43.
[35] Plantevin O., Glyde H. R., Fåk B., Bossy J., Albergamo F., Mulders N. and Schober H., *Phys. Rev. B*, **65** (2002) 224505.
[36] Glyde H. R., Albergamo F., Azuah R. T., Bossy J. and Fåk B., *Eur. Phys. J. E*, **12** (2003) 63.
[37] Albergamo F., Bossy J., Pearce J. V., Schober H. and Glyde H. R., *Phys. Rev. B*, **76** (2007) 064503.
[38] Bossy J., Pearce J. V., Schober H. and Glyde H. R., *Phys. Rev. Lett.*, **101** (2008) 025301.
[39] Plantevin O., Fåk B., Glyde H. R., Mulders N., Bossy J., Coddens G. and Schober H., *Phys. Rev. B*, **63** (2001) 224508.
[40] Albergamo F., Bossy J., Averbuch P., Schober H. and Glyde H. R., *Phys. Rev. Lett.*, **92** (2004) 235301.
[41] Pearce J. V., Bossy J., Schober H., Glyde H. R., Daughton D. R. and Mulders N., *Phys. Rev. Lett.*, **93** (2004) 145303.
[42] Chan M. H. W., Blum K. I., Murphy S. Q., Wong G. K. S. and Reppy J. D., *Phys. Rev. Lett.*, **61** (1988) 1950.
[43] Yamamoto K., Nakashima H., Shibayama Y. and Shirahama K., *Phys. Rev. Lett.*, **93** (2004) 075302.
[44] Taniguchi J., Aoki Y. and Suzuki M., *Phys. Rev. B*, **82** (2010) 104509.
[45] Yamamoto K., Shibayama Y. and Shirahama K., *Phys. Rev. Lett.*, **100** (2008) 195301.
[46] Glyde H. R., Azuah R. T. and Stirling W. G., *Phys. Rev. B*, **62** (2000) 14337.
[47] Sakhel A. R. and Glyde H. R., *Phys. Rev. B*, **70** (2004) 144511.
[48] Pearce J. V., Azuah R. T., Fåk B., Sakhel A. R., Glyde H. R. and Stirling W. G., *J. Phys.: Condens. Matter*, **13** (2001) 4421.
[49] Stirling W. G., *Recent High-Resolution Neutron Scattering Studies of Liquid ^{4}He*, in *Proceedings of Excitations in Two-Dimensional and Three Dimensional Quantum Fluids*, edited by Wyatt A. and Lauter H. J. (Plenum Press, New York) 1991, p. 25.